# Bio-Inspired Elastic Liquid-Infused Material for On-Demand Underwater Manipulation of Air Bubbles

Zhang, Jianqiang; Liu, Peng; Yi, Bo; Wang, Zhaoyue; Huang, Xin; Jiang, Lei; Yao, Xi

**Published in:**
ACS Nano

**Published: 24/09/2019**

**Document Version:**
Post-print, also known as Accepted Author Manuscript, Peer-reviewed or Author Final version



**Published version (DOI):**
10.1021/acsnano.9b04771

**Publication details:**
Zhang, J., Liu, P., Yi, B., Wang, Z., Huang, X., Jiang, L., & Yao, X. (2019). Bio-Inspired Elastic Liquid-Infused Material for On-Demand Underwater Manipulation of Air Bubbles. *ACS Nano*, *13*(9), 10596-10602. Advance online publication. https://doi.org/10.1021/acsnano.9b04771

# Bio-inspired Elastic Liquid-infused Material for On-demand Underwater Manipulation of Air Bubbles

*Jianqiang Zhang[†], Peng Liu[†], Bo Yi[†], Zhaoyue Wang[†], Xin Huang[†], Lei Jiang[#], Xi Yao[†,*]*

[†]Department of Biomedical Sciences, City University of Hong Kong, Tat Chee Avenue, Kowloon, Hong Kong SAR, PR China;

[#]Key Laboratory of Bio-inspired Smart Interfacial Science and Technology of Ministry of Education, School of Chemistry, Beihang University, Beijing 100191, PR China.

KEYWORDS

bubbles manipulation, bio-inspired, elastic liquid-infused material

ABSTRACT

Precise and robust manipulation of air bubbles will favor intense demands from governing processes of chemical reactions to enhancing transportation efficiency in multiphase engineering systems. Inspired by the working mechanism of mucous lining in lung alveoli, the elastic liquid-infused material (eLIM) is constructed by infiltrating an interconnected porous elastomer with a low-surface-energy lining liquid. With the help of the lining liquid, the pore pressure of the interconnected channels in eLIM can be reversibly regulated under mechanical stretching, balancing the capillary pressure in the channels with diverse radii and allowing gas flow in these channels. Therefore, air bubbles could be transported in and across the eLIM, showing on-demand control on the bubble contact angle, merging and splitting in an active and precise manner. The robust manipulation strategies on air bubbles can find applications in bioreactors and many other bubble-involved processes.

Dynamic manipulation of air bubbles in liquid environment is crucial in diverse animal behaviors.[1] For instance, diving bell spiders utilize hydrophobic hairs to trap air bubbles on their abdomens and legs for subaqueous living.[2] Some moles and water shrews use air bubbles to transport odorant for underwater olfaction.[3] A variety of industrial processes also substantially rely on the mass transfer and dynamic behaviors of bubbles in submerged substrate, such as water remediation,[4, 5] drag reduction,[6, 7] boiling heat transfer,[8] and electrolysis.[9, 10] Nevertheless, the kinetic motion of gas bubbles together with their hydrodynamics of gas-liquid interface complicate the bubble-substrate interactions, posing significant technical challenges to the precise and robust manipulation of air bubbles in those bubble involved systems and devices.

There are a couple of examples on the manipulation of air bubbles via materials with special surface chemistry and topography by taking advantages of the surface wettability regulated air bubble affinity as well as the topographical gradient induced asymmetric Laplace pressure on the air bubble.[11-14] These materials work well on trapping, collecting and transporting air bubbles in a range of diameters.[15] However, the drawbacks are also noticeable. On the one hand, environmental medium in submerged systems affect largely on the surface hydrophobicity/superhydrophobicity and thus may cause irreversible changes on air bubble affinity. For example, the superhydrophobic surfaces would lose the underwater gas affinity encountering either the degradation of air cushion or the contamination by surfactant.[16, 17] On the other hand, the effective length of topographical gradient on transporting air bubble is very limited, and air bubbles exceeding the length-scale of topographical gradient cannot generate sufficient shape distortion and thus Laplace pressure to trigger the motion.[18] Therefore, it is highly desirable on designing materials to enable robust manipulation strategies on air bubbles in aqueous mediums.

Natural systems are commonly operated in dynamic ways adapting to environmental changes. Particularly, among the human respiratory process, continuous and efficient gas exchanges would take place in the lung,[19] which contains millions of interconnected and elastic alveoli with diameters around 200 to 300 μm. At such length scale, the broad size distribution on alveolus results in huge difference on Laplace pressure of the encapsulated air bubbles. To enable simultaneous and uniform inhalation and exhalation of all alveoli, a layer of mucous surfactant lines out of each alveolus, lowering and balancing the surface tension of alveoli and enabling smooth gas flow in the lung (Figure 1a).[20] Meanwhile, the lining layer protects the alveoli tissue from direct contact of dust and other airborne contaminants.[21-24] The synergy of these features enables the robust gas exchange and adaptive function of the human pulmonary system in diverse climates.

Inspiring from the working mechanism of alveoli and mucous lining, we herein report a mechano-adaptive material – namely 'elastic liquid-infused material' (eLIM) – for on-demand underwater manipulation of air bubbles. Our system shares the key features as alveoli that air bubbles could be impregnated into the eLIM and then transported through the interconnected pores and channels along with the distribution of low-surface-energy lining liquid, which will further allow on-demand control on the bubble contact angle, merging and splitting in an active and precise manner. Furthermore, the immiscibility of low-surface-energy lining liquid also grants a self-cleaning feature to eLIM to enable robust function in diverse conditions. All these make eLIM a promising platform in areas where air bubble manipulation is instrumental including chem/bioreactors, fermentation, catalysis, and electrolysis.

## RESULTS AND DISCUSSION

The bio-inspired eLIM could be constructed by infiltrating an elastic interconnected porous substrate with a low-surface-energy liquid – the infused liquid should wet the porous substrate in submerged conditions and can bear readily redistribution under mechanical deformation of the substrate.[25-27] In accordance with the alveolar system, bubble manipulation via eLIM is based on both the elastic deformation of the substrate and the capillary action due to the reconfiguration of the infused liquid (Figure 1b). When operating underwater, bubble sitting on the surface of eLIM could invade along with the expansion of substrate and with the redistribution of the infused liquid. When the applied strain is released, the captured bubble also could be squeezed out with the contraction of the substrate and with the back flow of the infused liquid. The mechanism could be explained well by considering the eLIM system as a modeled poroelastic material.[25] In this regard, when stress is generated onto the porous substrates, the pore-fluid pressure will decrease, with the pressure drop $\Delta P_S = -B\sigma$, where $\sigma$ is the stress sensed by the substrate and $B$ represents the incompressible constituent of the system.[25, 28, 29] Meanwhile, the interface of infused liquid will cave inwards porous channels to balance $\Delta P_S$ by Laplace pressure $\Delta P_L = 2\gamma_l/r_m$, where $\gamma_l$ is the interfacial tension of infused liquid/gas and $r_m$ is the radius of meniscus curvature (Figure 1b).[30] Therefore, by stretching the eLIM in submerged conditions, the change of pore pressure, liquid redistribution and air bubble transportation are highly interactive and could happen simultaneously. Similar to the lining mucus of alveolar system, a low-surface-energy liquid could effectively decrease the overall magnitude of the Laplace pressure of pores with diverse radii in the eLIM. Effective inflation of the interconnected pores and channels could be performed at low operating stress, enabling maximal accommodation of air cushion inside the eLIM and thus the capability of on-demand bubble manipulation.

To realize the eLIM, porous matrix was fabricated by thermal curing silicone elastomer with a sacrificial template method. Sodium chloride (NaCl) powders as template were added into glass mould, followed by infusing a silicone precursor (SYLGARD 184) diluted by ethyl acetate (Figure S1). After curing the precursor and dissolving the NaCl, elastic porous silicone was obtained (Figure 1c). The structure, morphology and mechanics of the porous silicone can be controlled by adjusting the size and filling ratio of NaCl powders (Figure S2). In this work, the optimal Young's modulus of the porous silicone is ~120 kPa with an average pore size at 60 μm and 50% porosity, and the maximum strain can be up to 80% with 0.15 MPa for sample membrane at 1 mm thickness, respectively. Such porous silicone is hydrophobic in air and shows high bubble affinity when it is put underwater – a deposited air bubble will spread and vanish quickly on the surface. A perfluoro-lubricant (Fomblin, average molecular weight, 1800) was selected as infusing liquid, due to the low surface energy (17.1 mN/m) and excellent stability to cover the porous substrate in water (Figure S3).[16, 31] Moreover, this perfluoro-lubricant is no cytotoxicity and even stable in submerged, extreme pH, salinity, and UV environments.[32,33] The eLIM was finally obtained by adjusting the infusing amount of the perfluoro-lubricant on to the porous silicone (Figure S4).

ELIM exhibits a characteristic strain-dependent pore volume change and lubricant redistribution under mechanical deformation, which validates our discussed poroelastic model previously. When uniaxial stress is gradually applied, the pores and channels of the substrate are expanded accordingly, and infused lubricant is reconfigured along the channels in the stretched substrates. To better characterize pore volume change, the ratio of pore volume ($V_p$) to the matrix volume ($V_m$) of eLIM is thus defined as void ratio ($V_p/V_m$). Figure 1d shows that the void ratio of eLIM filling with 20 μL/cm$^2$ lubricant changes gradually and reversibly with the applied strain,

which is fundamental in the manipulation of air bubbles. Moreover, Figure 1e shows a connective performance of air bubbles on the eLIM sample under strain 0% and 40%. At relaxing state, the air bubbles keep stationary, because pores and channels are blocked by infused lubricant. At strain 40%, the stretched eLIM could mediate the transportation of the small bubble to the big one under unbalanced Laplace pressure, because the pores and channels are reconnected with the redistribution of the infused lubricant under strain (Movie 1).

Unlike other reported systems, eLIM shows robust, continuous and reversible tunability on the configuration and the contact angles of depositing air bubbles. As shown in Figure 2a, on a typical sample of 20 μL/cm$^2$ infused lubricant, BCA of a 3 μL air bubble changes gradually from 85° to 5° with growing strain from 0% to 20% and it can fully recover when the strain is released (Movie 2). The change of BCA is subject to the configuration of the distribution of the infused lubricant. Furthermore, parametric studies reveal that the sensitivity (ratio of the change of BCA to the applied strain) of the strain-based adjustment can be precisely controlled by simultaneously tuning the amount of infused lubricant and the size of the probing air bubble (Figure 2b and c). For example, for the same BCA change, eLIM infused with more lubricant needs larger strains to generate sufficient void volume to accommodate the air bubble, and smaller air bubbles are much easier to be impregnated into the eLIM.

The tunability on BCA is robust and the eLIM system can maintain function in multiple repeating cycles (Figure 2d). This is ascribed to the synergetic effect of excellent elasticity of the porous substrate, the flowability of the infused lubricant and its immiscibility to environmental medium. Wettability of the liquid-infused substrate is not altered after multiple repeating cycles performed in water. As a comparison, when bare porous substrate (without infusing lubricant) is put in water, the trapped air cushion in the substrate will be replaced by surrounding water

shortly (Figure S6). Actually, current superhydrophobic bubble-manipulating materials are limited to the robustness in submerged conditions, because they are likely to be impregnated by water due to hydraulic pressure and gas diffusion.[16] All these results prove the robust and precise tunability of eLIM for bubble contact angles control.

The eLIM offers a platform for operating multi-bubble behaviors including transportation, merging and splitting. As shown previously in Figure 1e and here in Figure 3a, a fast and steady bubble merging can be performed based on the way of the strain applications. Initially, three bubbles with different radii are collected by eLIM with similar BCAs. As the strain gradually increases, gas bubbles steadily transport through the interconnected channels and are temporarily reserved in eLIM. As described previously, during the stretching, the pore pressure drops, and the bubble transportation and the lubricant redistribution happens simultaneously to accommodate the additional volume from the air bubbles. Therefore, the volume of all three bubbles drops simultaneously. When a larger strain is reached, the smallest bubble completely impregnates into the eLIM, and two caps are left for the bubbles of larger volume (Movie 3). As eLIM snaps back in tension, the pore pressure is removed and the trapped air cushion moves outwards, forming a water-gas cap again; then the Laplace pressure at water-gas interface will increase until an equilibrium state is reached. It is worth noting that all air cushion trapped in the interconnected channels will only be propelled outside eLIM from the water-gas interface site with a smaller Laplace pressure, resulting in the merging of multiple bubbles.

To enable multipurpose and precise manipulation of air bubbles, the eLIM can be further engineered with patterns of controlled geometry and porosity to adjust the mechanic response and thus control the pore pressure and capillary pressure sensed in the system. As illustrated in Figure 3b, a radial hollowed region (radius: 0.5 mm, depth: 0.5 mm) is fabricated to induce a

thinner thickness on the porous substrate, and a non-uniform strain distribution will be thus generated when stretching the eLIM sample: the thinner thickness at the hollowed region will respond with a higher strain and thus a larger pore deformation during the stretching process, comparing to the surrounding region. Therefore, when the stress is relaxed, the reserved gas in the eLIM will escape from the thinner region where the curvature is smaller. A bubble will be precisely transported from any site to the patterned site (Movie 3). Similarly, this strategy can be used in transmembrane merging and splitting of bubbles. As shown in Figure 3c, two smaller bubbles sitting on eLIM can first impregnate into the eLIM during the stretching and a bigger bubble is generated at the patterned sites on the other side of the substrate during the relaxing. As shown in Figure 3d, bubble-splitting manipulation can also be observed by adjusting the patterned sites. It is worth noting that there is almost no change on the bubble volume before and after the transportation, merging and splitting process, indicating strong reliability of our system, which results from low-surface-energy infused lubricant (Figure S7).

Here we demonstrate the application of eLIM as adjustable pressure-limiting valve for controlling excessive gas bubbles in multiphase system. Controllable release of excessive bubbles is crucial in diverse engineering systems, such as chem/bioreactors, fermentation and wastewater treatment. One of the main challenges associated with releasing bubbles is that it requires sophisticated pressure-limiting valve that is expensive and susceptible to contamination. Thus, we suggest eLIM with robust and on-demand bubble manipulation capability for controlling excessive bubbles in a proof-of-concept bacterial reactor. As a demonstration, a glass chamber filled with culture medium containing *Escherichia coli* (*E. coli*) is connected to air inlet and pressure sensor, with the other end mounted and sealed with an eLIM membrane (Figure 4a). Under constant flow ventilation, bubbles gather on eLIM and the internal pressure of the

chamber gradually increases, resulting in mechanical stretching of eLIM membrane (Figure 4b). With the increase of the internal pressure, the gradual stretching of eLIM membrane will facilitate bubble transportation cross the membrane (Figure S8). The escaping of excessive bubbles from the chamber results in the regulation of the internal pressure, during which the eLIM membrane serves as a pressure-limiting valve. In addition, because of the presence of low-surface-energy lubricant, eLIM was granted self-cleaning feature. To demonstrate this self-cleaning function, we monitored the bacterial fouling on eLIM and porous polytetrafluoroethylene (ePTFE) membrane, respectively. It could be found that, compared with traditional hydrophobic ePTFE membrane, eLIM membrane exhibits no detectable residue of *E. coli* after culture (Figure 4c).

Actually, the ability on pressure regulation by the eLIM-based pressure-limiting valve is highly controllable. In our system, the critical pressure ($\Delta P_C$) for releasing bubbles is subject to Laplace pressure ($\Delta P_L$) of infused liquid meniscus and pressure ($P_E$) deriving from deformed eLIM. Therefore, the $\Delta P_C$ can be described as follow:

$$\Delta P_C = \Delta P_L + P_E \sim 2\gamma_l/r_p + 2Eh(\theta - \sin\theta)/R$$

$R$ is the radius of the eLIM membrane mounted chamber and $E$, $h$, $2\theta$, $r_p$ is elastic modulus, thickness, bend angle and pore radius of the eLIM membrane, respectively (Figure S8). Consequently, the critical pressure can be rationally adjusted by tuning the above mentioned parameters individually or simultaneously in the eLIM membrane. Indeed, Figure 4d and e prove that the critical pressure decreases with increasing pore radius and grows as increasing thickness of the eLIM membrane, which is consistent with the equation above.

**CONCLUSION**

In summary, a bio-inspired eLIM has been proposed and designed to mimic the features and functions of the alveolar system in manipulating air bubbles in submerged conditions. The eLIM is realized by infiltrating porous silicone with low-surface-energy perfluoro-lubricant to enable stable overcoat on the porous silicone and reversible distributing under mechanical regulation in aqueous solution. Our results show that eLIM presents a conceptual strategy to manipulate bubbles, which is mainly dependent on the reversible adaption of the infused liquid-gas interface for responsive deformation of substrate. Therefore, in eLIM system the bubble manipulation will be independent on interface wettability of outside media, endowing manipulation strategy with precision and universality. This stimulus-triggered eLIM will favor intense demands in membrane separation, fermentation, medical devices, biomedical fluid handling, multiphase chemical and biochemical reactions, where both advanced membrane technique and on-demand gas bubble manipulation are highly desired.

## EXPERIMENTAL SECTION

**Fabrication of elastic liquid-infused material (eLIM).** Firstly, sodium chloride (NaCl) powders as template were added into glass mould. Then the mixture of silicone (Sylgard 184, Dow Corning Corporation, USA) precursor, curing agent and ethyl acetate at a weight ratio of 10:1:15 also were infused into this mould. In addition, this mixture of silicone/NaCl was cured at 70°C for 5 h. An elastic interconnected porous silicone was obtained by dissolving NaCl particles. Secondly, the perfluoro-lubricant (Fomblin, average molecular weight, 1800) was infused into the porous silicone to fabricate eLIM and tuned the infusing amount.

**Characterization of bubble manipulation.** Water contact angle and bubble contact angle were measured by OCA20 equipment (Data Physics, Germany) at room temperature, respectively. The eLIM stretching was carried out using a uniaxial stretcher, with a thread pitch of 0.6 mm. The

eLIM was mounted by screwed clippers on a pair of arms of the stretcher which is placed under water. And the snapshots of bubble manipulation were recorded at 30 frames per second (fps).

**Antifouling property of eLIM membrane.** Green fluorescent protein (GFP)-tagged *Escherichia coli* (*E. coli*) was cultured in 30 mL of LB broth. The antifouling test was studied by sealing open end of culture chamber with eLIM and ePTFE (average pore size of 0.2 μm, Sterlitech) membrane, respectively. During this culture, LB broth containing *E. coli* was injected air bubbles resulting in droplets splashing on eLIM or ePTFE membrane. After culture, the treated eLIM and ePTFE membrane were slightly washed with deionized water and then stained with dye SYTO 9 in PBS solution for 20 min. Whereafter, adhered *E. coli* on the eLIM and ePTFE membrane were detected by Nikon Eclipse Ni-E fluorescent microscope with an excitation of 488 nm.

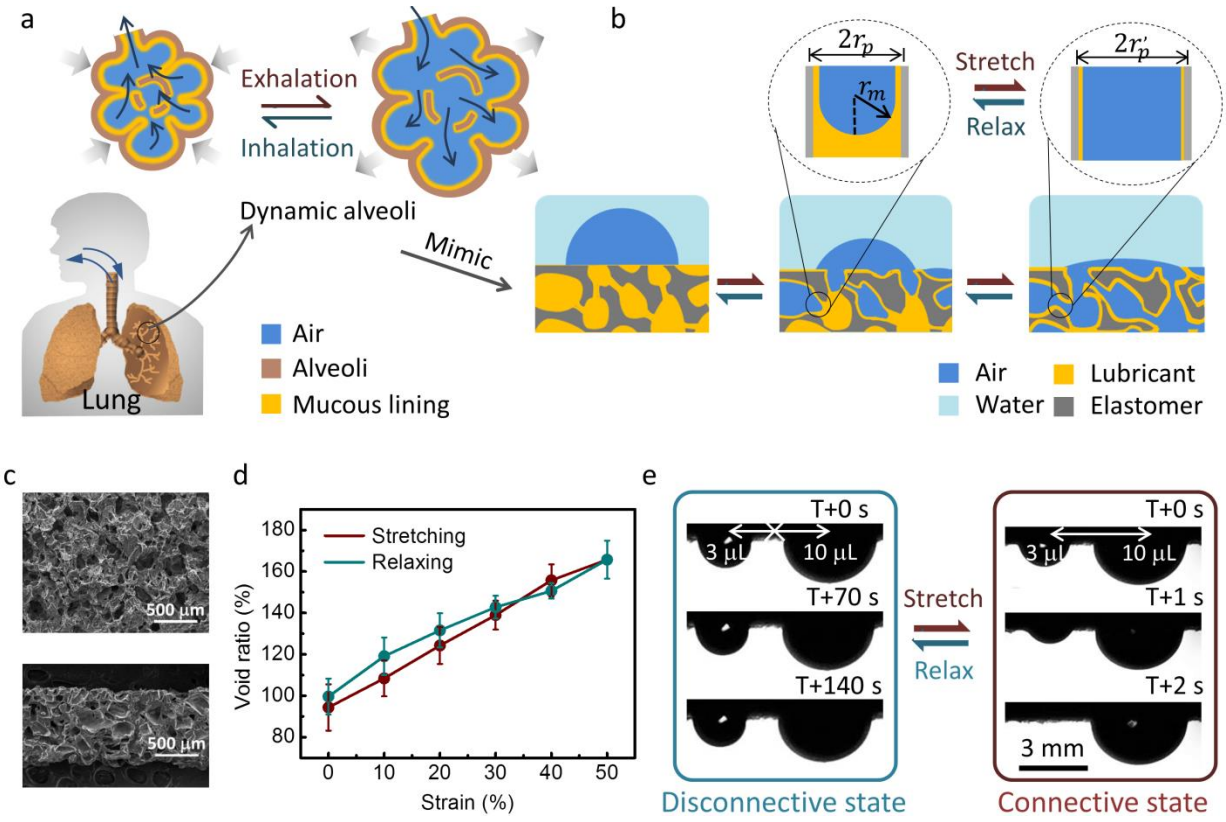


**Figure 1.** Bio-inspired design of elastic liquid-infused material (eLIM). (a) Scheme illustrating the spontaneous inhalation and exhalation of alveoli with different radius with the assistance of mucous lining. (b) Inspired by alveoli, eLIM is designed to manipulate bubble by mechanical stimulation. Under an increased tension, air bubble on eLIM begins to invade into the expanded pores and channel. When the applied tension is removed, the bubble is squeezed out with the recovery of the elastic substrate. (c) Top and cross-section SEM images of the porous silicone substrate show interconnected porous architecture. (d) The change of void ratio ($V_p/V_m$) of eLIM as a function of applied strains. The perfluoro-lubricant is applied at 20 μL/cm$^2$. (e) Snapshots showing the bubble transportation in eLIM resulting from stretch-induced liquid redistribution and the corresponding pore connectivity. The eLIM membrane is blocked by infused liquid at relaxing state, and is permeable when 40% strain is applied. And the white arrow represents the connectivity performance of pore and channel in eLIM.

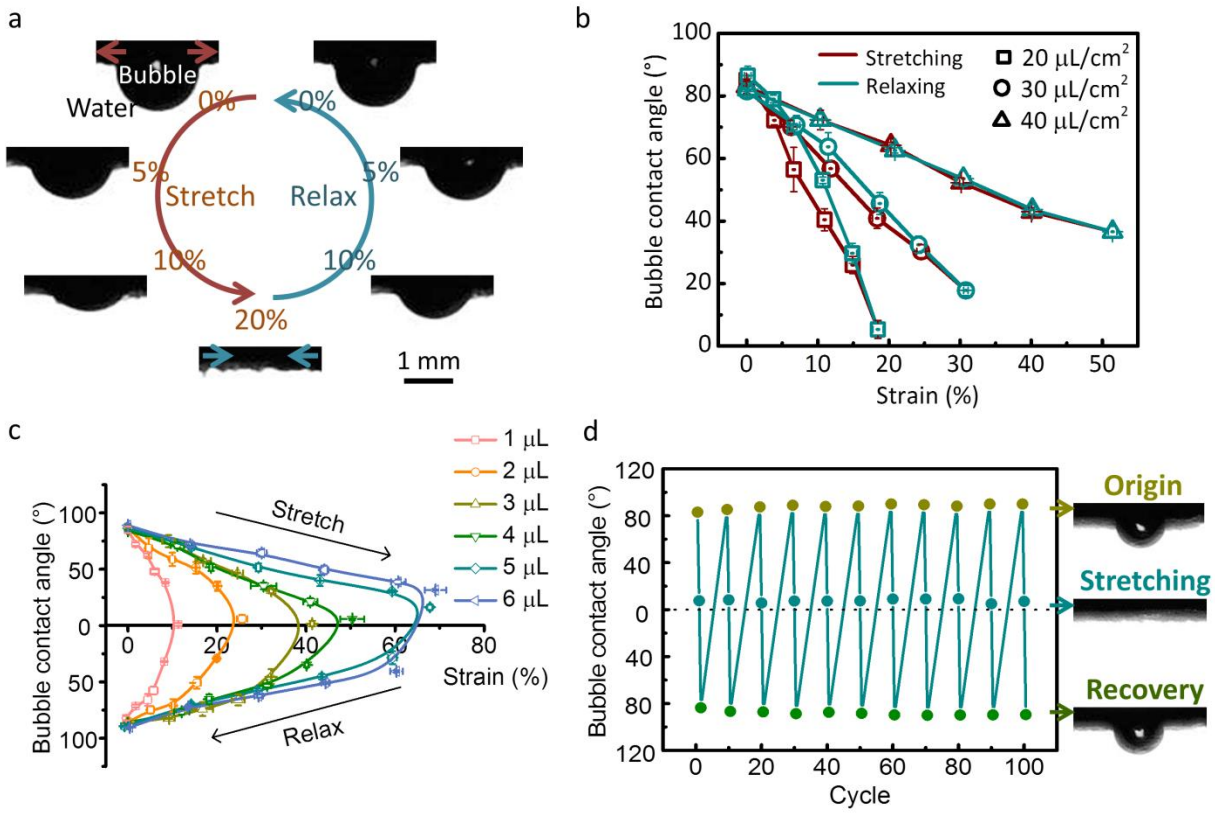


**Figure 2.** Reversible tunability on bubble contact angles. (a) Optical snapshots showing the shape evolution of air bubble (3 μL) on eLIM (20 μL/cm$^2$ perfluoro-lubricant) under varying strains. (b) Comparison of BCA as a function of applied strains on the eLIM filling with different amounts of lubricant. 3 μL air bubble is used in the tests. (c) Tuning the BCA as a function of strain for different bubble volumes (1 μL ~ 6 μL). (d) Repeating test on the BCA after 100 cycles. 2 μL air bubble is used and a maximum 20% strain is applied, respectively.

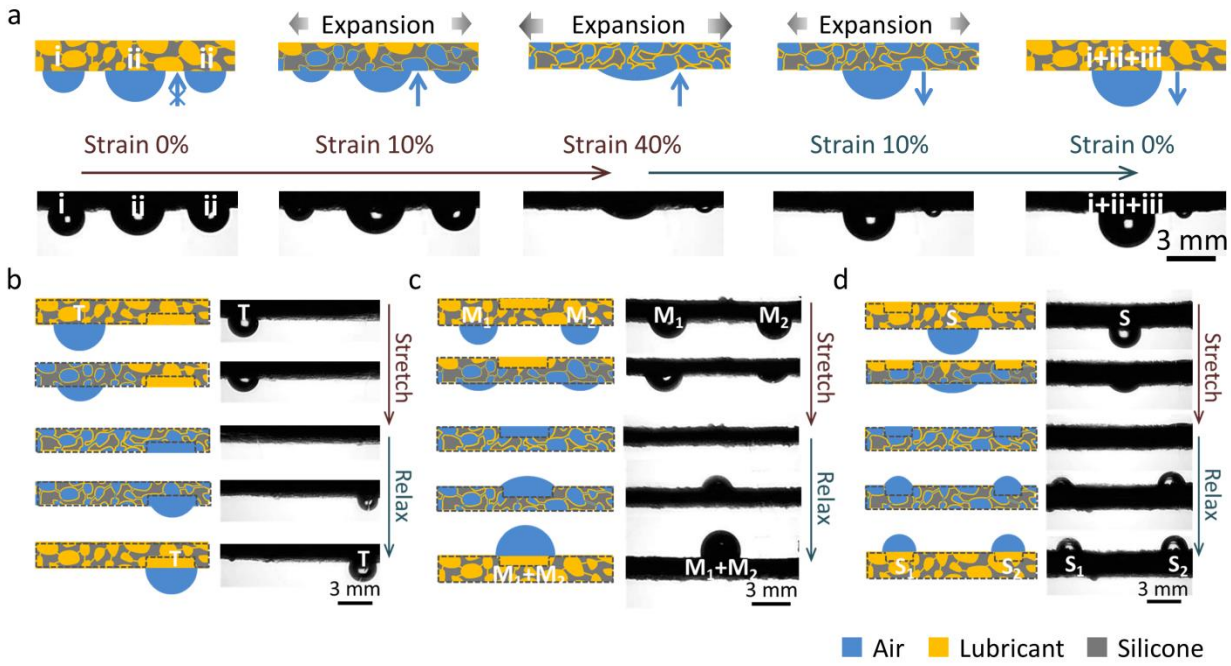


**Figure 3.** On-demand merging and splitting of air bubbles. (a) Scheme showing the merging mechanism of bubbles: two independent bubbles were both temporarily impregnated into eLIM membrane and then squeezed out as one bubble by stretching stimulation. The snapshots validate this hypothesis of bubble merging. The volume of bubble i, ii and iii is 2 μL, 4 μL and 2 μL, respectively. (b) Scheme showing the progress of applying eLIM for transporting gas bubble from any sites to the patterned site where the Laplace pressure is smaller. The snapshots validate this hypothesis. The volume of bubble T is 2 μL in snapshots. (c) Scheme showing the manipulation progress of transmembrane bubble merging on patterned site. The snapshots validate this hypothesis. The volume of bubble $M_1$ and $M_2$ is 2 μL in snapshots, respectively. (d) Scheme showing the dynamic process of transmembrane bubble splitting. The snapshots validate this hypothesis. The volume of bubble S is 2 μL.

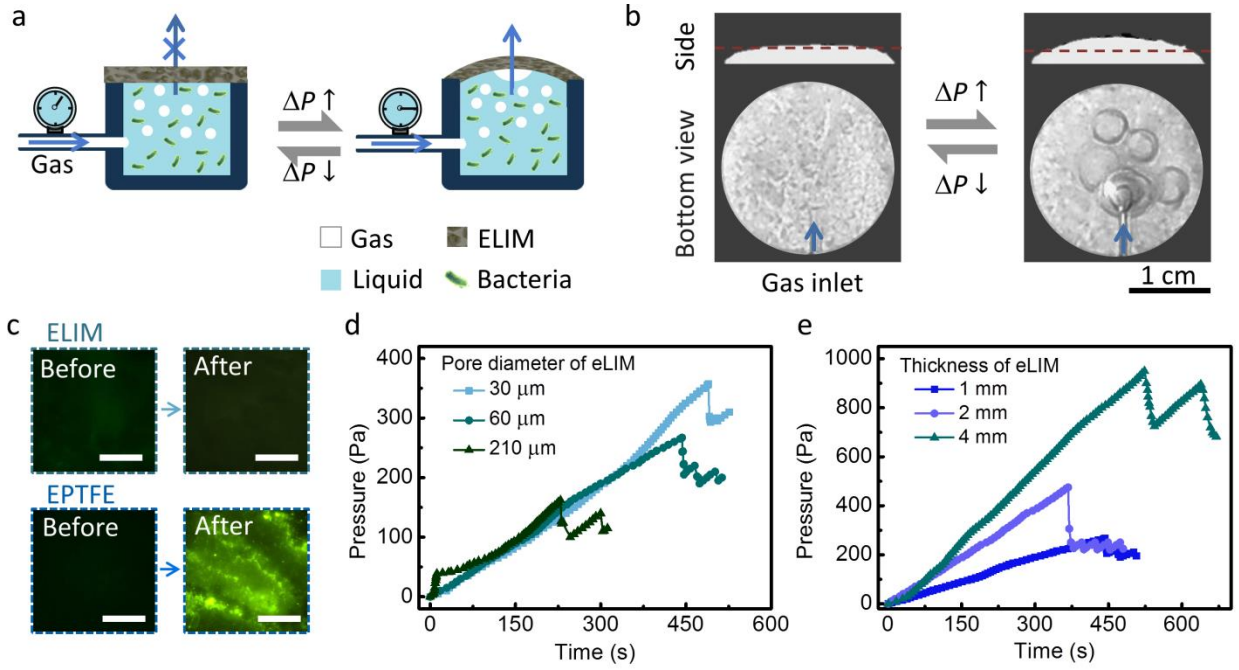


**Figure 4.** ELIM as adjustable pressure-limiting valve. (a) Scheme showing the eLIM-based pressure-limiting valve for controlling excessive bubbles in bacterial reactor. (b) Snapshots demonstrating the mechanical stretching of eLIM membrane under the action of air pressure (side view). Excessive air bubbles will accumulate at the eLIM membrane before they could escape. (c) Antifouling properties of eLIM and ePTFE membrane before and after bacterial culture. No adhension of *E. coli* is observed on eLIM membrane after culture. A significant amount of residual *E. coli* is left on ePTFE membrane. Scale bar is 200 μm. (d) The time-dependent pressure changes of the chamber by using eLIM membranes with different porosity. The critical pressure of the eLIM-based pressure-limiting valve decreased with the increase of the pore size in the membrane. (e) The time-dependent pressure changes of the chamber by using eLIM membranes with different thickness. The critical pressure increased with the growth of the membrane thickness.

## ASSOCIATED CONTENT

The Supporting Information is available free of charge on the ACS Publications website.

Experimental details and additional characterization data (SEM images, stress–strain curves, water and bubble contact angle, bubble volume change) (PDF)

Movie 1: the connectivity changes of eLIM channels with different strains (AVI)

Movie 2: reversible tunability on bubble contact angles (AVI)

Movie 3: on-demand transportation, merging and splitting of air bubbles (AVI)

## AUTHOR INFORMATION

Corresponding Author

* E-mail: xi.yao@cityu.edu.hk

### Author Contributions

X.Y. conceived the concept and supervised the research. X.Y., L.J., and J.Z. designed the experiments. J.Z. and P.L. performed the research. B.Y., Z.W. and X.H. supported material characterization. X.Y. and J.Z. wrote the manuscript.

### Notes

The authors declare no conflict of interest.

## ACKNOWLEDGMENT

The authors thank the financial support by the General Research Fund (GRF) Hong Kong (Grant No. 11274616), the Collaborative Research Fund (CRF) Hong Kong (Grant No. C1018-17G) financial support from City University of Hong Kong and Shenzhen Basic Research Program (JCYJ20180307123925200).

REFERENCES

(1) Stride, G. O. The Respiratory Bubble of the Aquatic Beetle, Potamodytes Tuberosus, Hinton. *Nature* **1953,** *171*, 885.

(2) Neumann, D.; Woermann, D. Stability of the Volume of Air Trapped on the Abdomen of the Water Spider Argyroneta Aquatica. *SpringerPlus* **2013,** *2*, 694.

(3) Catania, K. C., Olfaction: Underwater 'Sniffing' bySemi-aquatic Mammals. *Nature* **2006,** *444*, 1024.

(4) Camel, V.; Bermond, A. The Use of Ozone and Associated Oxidation Processes in Drinking Water Treatment. *Water Res.* **1998,** *32*, 3208-3222.

(5) Siddiqui, M. S.; Amy, G. L.; Murphy, B. D. Ozone Enhanced Removal of Natural Organic Matter from Drinking Water Sources. *Water Res.* **1997,** *31*, 3098-3106.

(6) Madavan, N.; Deutsch, S.; Merkle, C. Reduction of Turbulent Skin Friction by Microbubbles. *Phys. Fluids* **1984,** *27*, 356-363.

(7) Lu, J.; Fernández, A.; Tryggvason, G. The Effect of Bubbles on the Wall Drag in A Turbulent Channel Flow. *Phys. Fluids* **2005,** *17*, 095102.

(8) Son, G.; Dhir, V.; Ramanujapu, N. Dynamics and Heat Transfer Associated with A Single Bubble during Nucleate Boiling on A Horizontal Surface. *Journal of Heat Transfer* **1999,** *121*, 623-631.

(9) Lu, Z.; Zhu, W.; Yu, X.; Zhang, H.; Li, Y.; Sun, X.; Wang, X.; Wang, H.; Wang, J.; Luo, J. Ultrahigh Hydrogen Evolution Performance of Underwater "Superaerophobic" $MoS_2$ Nanostructured Electrodes. *Adv. Mater.* **2014,** *26*, 2683-2687.

(10) Su, B.; Tian, Y.; Jiang, L. Bioinspired Interfaces with Superwettability: from Materials to Chemistry. *J. Am. Chem. Soc.* **2016,** 138, 1727-1748.

(11) Wang, J.; Zheng, Y.; Nie, F. Q.; Zhai, J.; Jiang, L. Air Bubble Bursting Effect of Lotus Leaf. *Langmuir* **2009,** *25*, 14129-34.

(12) Chang, F. M.; Sheng, Y. J.; Cheng, S. L.; Tsao, H. K. Tiny bubble removal by gas flow through porous superhydrophobic surfaces: Ostwald ripening. *Appl. Phys. Lett.* **2008,** 92, 264102.

(13) Chen, M. Y.; Jia, Z. H.; Zhang, T.; Fei, Y. Y. Self-transport of underwater bubbles on a microholed hydrophobic surface with gradient wettability. *Soft matter* **2018,** 14, 7462-7468.

(14) Yu, C.; Zhang, P.; Wang, J.; Jiang, L. Superwettability of Gas Bubbles and Its Application: from Bioinspiration to Advanced Materials. *Adv. Mater.* **2017,** *29*, 1703053.

(15) Ma, H.; Cao, M.; Zhang, C.; Bei, Z.; Li, K.; Yu, C.; Jiang, L. Directional and Continuous Transport of Gas Bubbles on Superaerophilic Geometry-gradient Surfaces in Aqueous Environments. *Adv. Funct. Mater.* **2018,** *28*, 1705091.

(16) Wong, T. S.; Kang, S. H.; Tang, S. K.; Smythe, E. J.; Hatton, B. D.; Grinthal, A.; Aizenberg, J. Bioinspired Self-repairing Slippery Surfaces with Pressure-stable Omniphobicity. *Nature* **2011,** *477*, 443-7.

(17) Lv, P.; Xue, Y.; Shi, Y.; Lin, H.; Duan, H. Metastable States and Wetting Transition of Submerged Superhydrophobic Structures. *Phys. Rev. Lett.* **2014,** 112, 196101.

(18) Zhang, C.; Zhang, B.; Ma, H.; Li, Z.; Xiao, X.; Zhang, Y.; Cui, X.; Yu, C.; Cao, M.; Jiang, L. Bioinspired Pressure-tolerant Asymmetric Slippery Surface for Continuous Self-transport of Gas Bubbles in Aqueous Environment. *ACS Nano* **2018,** *12*, 2048-2055.

(19) Namati, E.; Thiesse, J.; de Ryk, J.; McLennan, G. Alveolar Dynamics During Respiration: Are the Pores of Kohn A Pathway to Recruitment? *Am. J. Resp. Cell. Mol.* **2008,** *38*, 572-578.

(20) Pattle, R. E. Properties, Function, and Origin of the Alveolar Lining Layer. *Roy. Soc. B. Biol. Sci.* **1958,** *148*, 217-240.

(21) Thornton, D. J.; Sheehan, J. K. From Mucins to Mucus: toward A More Coherent Understanding of This Essential Barrier. *Proc. Am. Thorac. Soc.* **2004,** *1*, 54-61.

(22) Amini, S.; Kolle, S.; Petrone, L.; Ahanotu, O.; Sunny, S.; Sutanto, C. N.; Hoon, S.; Cohen, L.; Weaver, J. C.; Aizenberg, J. Preventing Mussel Adhesion Using Lubricant-infused Materials. *Science* **2017,** *357*, 668-673.

(23) Jiang, J.; Gao, J.; Zhang, H.; He, W.; Zhang, J.; Daniel, D.; Yao, X. Directional Pumping of Water and Oil Microdroplets on Slippery Surface. *Proc. Natl. Acad. Sci. USA* **2019,** *116*, 2482-2487.

(24) He, W.; Liu, P.; Zhang, J.; Yao, X. Emerging Applications of Bioinspired Slippery Surfaces in Biomedical Fields. *Chem. Eur. J.* **2018,** *24*, 14864-14877.

(25) Yao, X.; Hu, Y.; Grinthal, A.; Wong, T. S.; Mahadevan, L.; Aizenberg, J. Adaptive Fluid-infused Porous Films with Tunable Transparency and Wettability. *Nat. Mater.* **2013,** *12*, 529-34.

(26) Sheng, Z.; Wang, H.; Tang, Y.; Wang, M.; Huang, L.; Min, L.; Meng, H.; Chen, S.; Jiang, L.; Hou, X. Liquid Gating Elastomeric Porous System with Dynamically Controllable Gas/liquid Transport. *Sci. Adv.* **2018,** *4*, eaao6724.

(27) Hou, X.; Hu, Y.; Grinthal, A.; Khan, M.; Aizenberg, J. Liquid-based Gating Mechanism with Tunable Multiphase Selectivity and Antifouling Behaviour. *Nature* **2015,** *519*, 70-3.

(28) Rice, J. R.; Cleary, M. P. Some Basic Stress Diffusion Solutions for Fluid-saturated Elastic Porous Media with Compressible Constituents. *Rev. Geophys.* **1976,** *14*, 227-241.

(29) Biot, M. A. General Theory of Three-dimensional Consolidation. *J. Appl. Phys.* **1941,** *12*, 155-164.

(30) Scherer, G. W.; Smith, D. M. Cavitation during Drying of A Gel. *J. Non-Cryst. Solids* **1995,** *189*, 197-211.

(31) Zhao, B.; Pahlavan, A. A.; Cueto-Felgueroso, L.; Juanes, R. Forced Wetting Transition and Bubble Pinch-off in A Capillary Tube. *Phys. Rev. Lett.* **2018,** *120*, 084501.

(32) Li, J.; Kleintschek, T.; Rieder, A., Cheng, Y.; Baumbach, T.; Obst, U.; Schwartz, T.; Levkin, P. A. Hydrophobic liquid-infused porous polymer surfaces for antibacterial applications. *ACS Appl. Mater. Inter.* **2013,** *5*, 6704-6711.

(33) Epstein, A. K., Wong, T. S., Belisle, R. A., Boggs, E. M., Aizenberg, J. Liquid-infused structured surfaces with exceptional anti-biofouling performance. *Proc. Natl. Acad. Sci. USA* **2012,** *109*, 13182-13187.

For Table of Contents Only

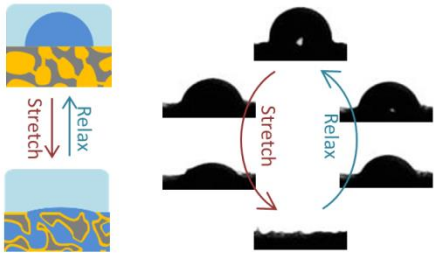


On-demand bubble manipulation